central hot point. This causes an axi-symmetric surface tension variation with a central minimum. Consequently, the surface profile gets deformed because of interplay of thermocapillary surface waves and internal gravity waves. The liquid is pulled out from the centre of the heated region and the depletion in the central region results in formation of a pit (fig. L.11.1). A careful analysis of the surface tension forces at the deformed liquid surface along with optical forces exerted by the incident laser beam, shows that these can lead to stable trapping of object in an annular region about the laser beam axis. It is pertinent to note here that the radiation pressure induced deformation of liquid surface is also present here and is expected to lead to a small bulging of the liquid surface along the beam axis. But such effect will be negligible compared to thermocapillary effect. Trapping of 2µm polystyrene microspheres with a 1064nm cw Nd:YAG laser beam (~ 40mW), focused with a low numerical aperture (0.5microscope) objective, is shown in fig. L.11.2. The trapped microspheres were imaged with a 40X objective lens and CCD camera. As can be seen in fig. L.11.2(a), initially the microspheres are trapped in an annular region about the laser beam axis. However, because of the convection flow, more microspheres are driven to the trap volume leading to a gradual build up of a cluster of the polystyrene microspheres. This approach could also be used for trapping of glass micro-rods and human red blood cells. The ability to manipulate microscopic objects near free liquid surface may prove valuable for several studies like for example, studies of colloidal dynamics at liquid-air interface, studies on crystalline thin-film structure of biomolecules like cholesterol at air/liquid interface etc.

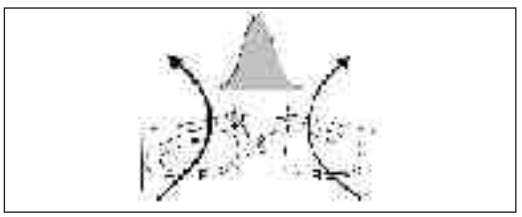

Fig. L.11. 1 *Trapping of microspheres at the free liquid surface, deformed by laser induced thermocappilarity. Dark arrows indicate optical forces and fade arrows indicate surface tension forces.*

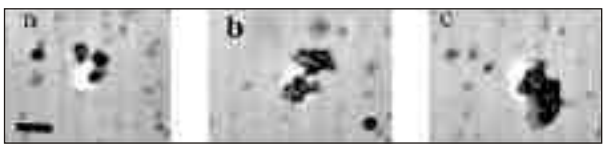

Fig. L.11.2 *Observation of trapping of 2µm polystyrene microspheres. (a) to (c) showing gradual accumulation of microsphers in the trap. Scale bar,10µm.*

Contributed by:
R. Dasgupta; raktim@cat.ernet.in, S. Ahlawat and P K Gupta

L.12 Active flux laser welding of austenitic stainless steel sheet

Active flux laser welding (ALW) process is being developed for austenitic stainless steel (SS) to produce narrower and deeper welds. The results of the laser welding (LW) study demonstrated that addition of flux (SiO_2) during LW caused significant reduction in the intensity and size of resultant plasma plume (fig. L.12.1). ALW was marked with large fluctuations in electron density of the plasma plume, which in turn, introduced fluctuations in the absorption of CO_2 laser radiation. ALW brought about significant modification in the shape of the fusion zones (FZ) to produce narrower and deeper welds than those made without flux. Flux-induced change in the shape of FZ was more marked in welds involving keyhole formation, although conduction-limited laser welds also carried signatures of flux-addition on its shape (fig. L.12.2). The most apparent difference in the case of deeper "ALW" welds was transformation of a typical "wine-glass" shaped fusion zones into a more uniformly tapered "V-shaped" fusion zones (fig. L.12.3). Active flux laser weldments exhibited lower ductility than those of bead-on-plate laser weldments.

Fig L.12.1 *Variation in plasma plume during laser welding of partly flux-coated SS sheet.*

Fig. L.12.2 *Comparison of conduction-limited welds produced by LW and ALW.*

Fig. L.12.3 *Comparison of key-hole welds produced by LW and ALW.*

Contributed by:
A. K. Nath; aknath@cat.ernet.in